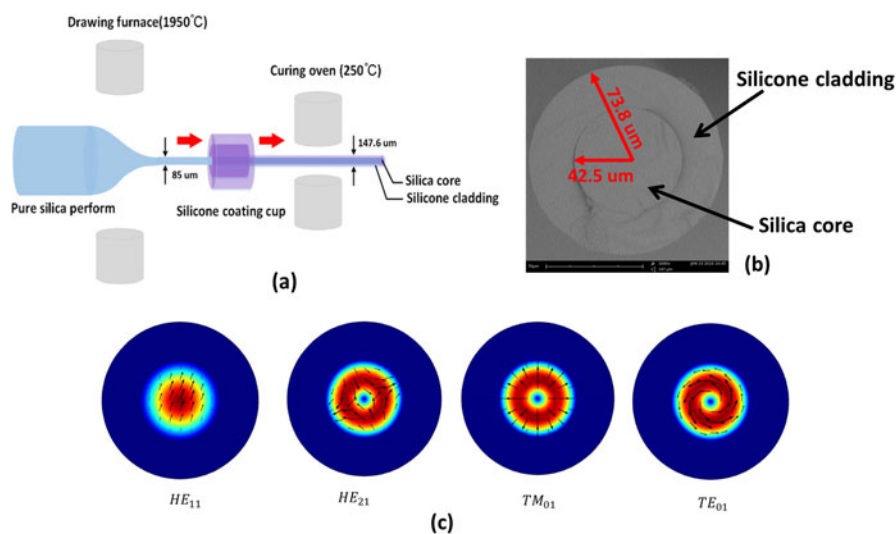


Highly Sensitive Small Pressure Monitoring Using Hyperelastic Silicone-Cladding/Silica-Core Composite Optical Fiber

Volume 9, Number 6, December 2017

Bin Zhou
Liang Wang
Lin Htein
Zhengyong Liu
Xiaolu Chen
Hwa-Yaw Tam, *Fellow, OSA*
Chao Lu, *Fellow, OSA*



DOI: 10.1109/JPHOT.2017.2779605
1943-0655 © 2017 IEEE

Highly Sensitive Small Pressure Monitoring Using Hyperelastic Silicone-Cladding/Silica-Core Composite Optical Fiber

Bin Zhou ^{1,2}, Liang Wang ³, Lin Htein,² Zhengyong Liu,²
Xiaolu Chen,¹ Hwa-Yaw Tam,² *Fellow, OSA*, and
Chao Lu ⁴, *Fellow, OSA*

¹Guangdong Provincial Key Laboratory of Optical Information Materials and Technology & National Center for International Research on Green Optoelectronics, South China Academy of Advanced Opto-electronics, South China Normal University, Guangzhou 510631, China

²Department of Electrical Engineering, The Hong Kong Polytechnic University, Hong Kong

³Department of Electronic Engineering, The Chinese University of Hong Kong, Hong Kong

⁴Department of Electronic and Information Engineering, The Hong Kong Polytechnic University, Hong Kong

DOI:10.1109/JPHOT.2017.2779605

1943-0655 © 2017 IEEE. Translations and content mining are permitted for academic research only. Personal use is also permitted, but republication/redistribution requires IEEE permission. See http://www.ieee.org/publications_standards/publications/rights/index.html for more information.

Manuscript received September 9, 2017; revised November 19, 2017; accepted November 30, 2017. Date of publication December 4, 2017; date of current version December 14, 2017. This work was supported in part by the Hong Kong Scholars Program under Grant XJ2014027, in part by the China Post-Doctoral Science Foundation under Grant 2016M590794, in part by the National Natural Science Foundation of China under Grants 61307053, 61377093, and 61435006, in part by Hong Kong RGC GRF under Grant PolyU 5208/13E, in part by the HK PolyU project (1-YW0S), in part by the Guangdong Provincial Key Laboratory of Optical Information Materials and Technology under Grant 2017B030301007, and in part by the MOE International Research Laboratory of Optical Information. Corresponding author: Liang Wang (e-mail: lwang@ee.cuhk.edu.hk).

Abstract: We have fabricated a composite optical fiber with hyperelastic silicone cladding and silica core, and demonstrated a simple and highly sensitive pressure sensor based on the light coupling between two such composite fibers twisted together. The hyperelastic silicone has very low Young's modulus which makes the fiber deformation easier even under small pressure and hence improves the light coupling and pressure sensitivity. Both simulation and experiment show that the light coupling based pressure sensor using the composite fibers is very sensitive to small pressure (e.g., several newtons) compared with those using conventional silica fibers and polymethyl methacrylate resin polymer fibers, which almost have no response to small pressure. With excellent sensitivity and fast response time ($\ll 1$ s), both static and dynamic side pressure have been successfully detected. The sensing configuration is simple without any complicated structures and would be a cost-effective candidate for highly sensitive small pressure monitoring.

Index Terms: Fiber-optic pressure sensor, fiber fabrication, silicone-cladding/silica-core composite optical fiber, Young's modulus.

1. Introduction

Due to the advantages of immunity to electromagnetic interference, high sensitivity, low cost and small size, optical fiber sensors have been widely used in many fields, e.g., civil engineering, industrial production, national defense etc [1]. Parameters such as refractive index, pressure, strain,

temperature, humidity etc can all be measured by using fiber sensors [2]–[5]. For pressure sensing, various fiber structures like fiber Bragg gratings (FBG) [2], [6], fiber interferometers [7], [8] and tapered fibers [9], [10] have been proposed and demonstrated. Conventional optical fibers with silica cladding and core have been used to realize those structures. However silica is a hard material with high Young's modulus and thus the stiffness of the silica fiber makes it difficult to be deformed and compressed, leading to low pressure sensitivity [11]. To improve the pressure sensitivity, silica FBGs were embedded in polymer materials, e.g., polycarbonate [12] and silicon rubber [13], as they have relatively low Young's modulus and hence the pressure sensitivity can be increased. Later with the development of polymer optical fiber whose Young's modulus is lower than silica fiber, pure polymer FBGs have been fabricated and demonstrated to offer higher pressure sensitivity compared with silica FBGs [11], [14]–[16].

However, the Young's modulus of conventional polymer optical fiber made by Polymethyl Methacrylate Resin (PMMA) is still large, limiting further improvement of the pressure sensitivity. Moreover, the relatively high loss makes PMMA polymer fiber not suitable in long-distance sensing. In this paper we fabricate a hyperelastic silicone-cladding/silica-core composite optical fiber and develop a simple and highly sensitive pressure sensor based on it. Silica is used as the material of the fiber core, while hyperelastic silicone (Sylgard184, Dow Corning Ltd.) with very low Young's modulus, is used as the cladding material. Two such composite fibers are twisted together such that light coupling between them takes place when external pressure deforms the soft silicone claddings and makes the silica cores approach each other. By simply measuring the light intensity coupled from one fiber to the other, we can monitor the pressure applied to the fiber. The use of hyperelastic silicone as the cladding material gives rise to high sensitivity because the cores of the composite fibers can be more easily compressed closely to enhance the light coupling. And silica core offers lower loss than polymer fiber. Moreover, no post-processing of the fiber to form particular fiber structures like FBGs and interferometers etc is needed, which simplifies the sensing configuration. It is worth mentioning that hyperelastic organic silicon materials, e.g., polydimethylsiloxane and silicone etc, have been recently used in developing soft electronic skin and skin-like pressure sensors for highly intuitive human-computer user interfaces due to their flexibility and biocompatibility [17]–[20].

2. Fiber Fabrication and Experiment Setup for Small Pressure Monitoring

Fig. 1(a) depicts the fabrication process of the hyperelastic silicone-cladding/silica-core composite optical fiber used in the experiment by using fiber drawing tower. Note that the figure is plotted along horizontal direction for convenience. The pure silica preform is heated up to 1950 °C in the furnace and then is drawn into optical fiber with core diameter of 85 μm . The coating material is silicone (Sylgard184, Dow Corning Ltd.), which is mixed with curing agent at a weight ratio of 10:1. During the coating process, the pure silica core passes through the coating cup filled with mixed silicone and curing agent. As the surface tension of the silicone is low (20.4 mN/m for Sylgard184), coating silicone to the surface of pure silica core becomes easy. After this process, pure silica core is coated with a thin liquid silicone film. Finally the coated fiber immediately passes through a curing oven with temperature kept at 250 °C. The process takes 10 second and the liquid silicone is completely cured during that time. Fig. 1(b) shows the Scanning Electron Microscope (SEM) photo of the fabricated silicone/silica composite optical fiber. The core and cladding radii of the composite fiber are 42.5 μm and 73.8 μm , respectively. At 1550 nm region the refractive index of silicone and silica are 1.40 and 1.45, and the composite fiber supports multimode transmission. Fig. 1(c) depicts the field distribution of the fundamental mode and several higher-order modes inside the composite fiber. The attenuation coefficient of the composite fiber is measured to be 23 dB/km at 850 nm and 83 dB/km at 1550 nm. Compared with the loss of POF which is around the level of 100 dB/km at visible light region (below 650 nm) and much larger than 100 dB/km beyond 850 nm [21]–[24], the loss of our composite optical fiber is quite low. The thermo-optic coefficient for the silicone cladding of the composite fiber is negative, i.e., $-4.5 \times 10^{-4} / ^\circ\text{C}$, whose magnitude is about 2 orders larger than $8.6 \times 10^{-6} / ^\circ\text{C}$ of silica [25], [26]. The optical power distribution of the modes

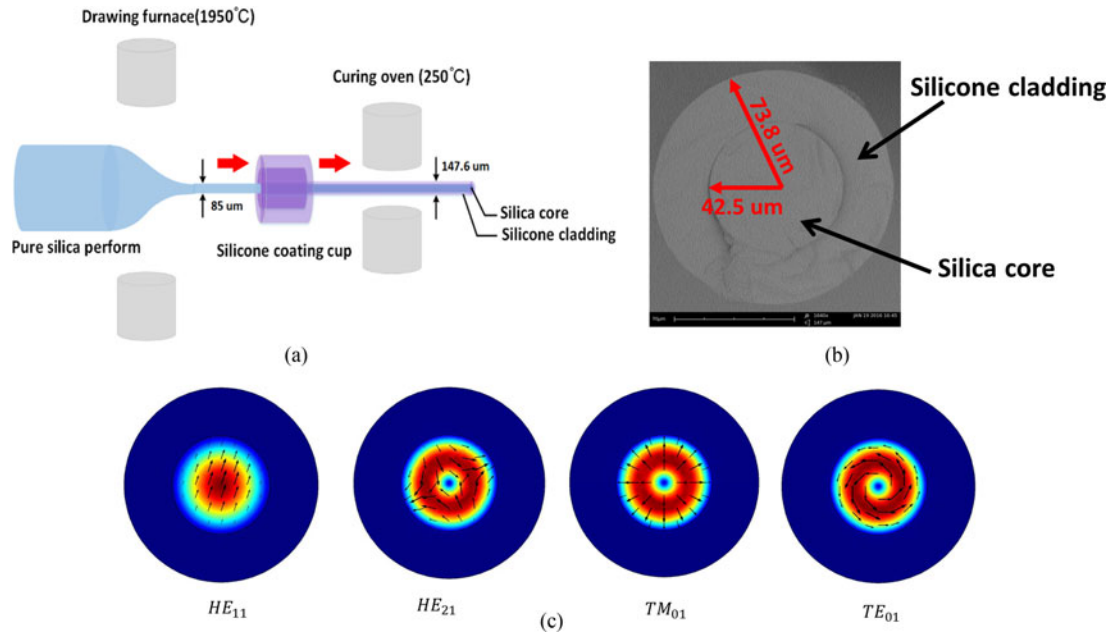


Fig. 1. (a) Fabrication of silicone-cladding/silica-core composite optical fiber; (b) Scanning Electron Microscope photo of the fabricated composite fiber; (c) field distribution of several modes inside the composite fiber.

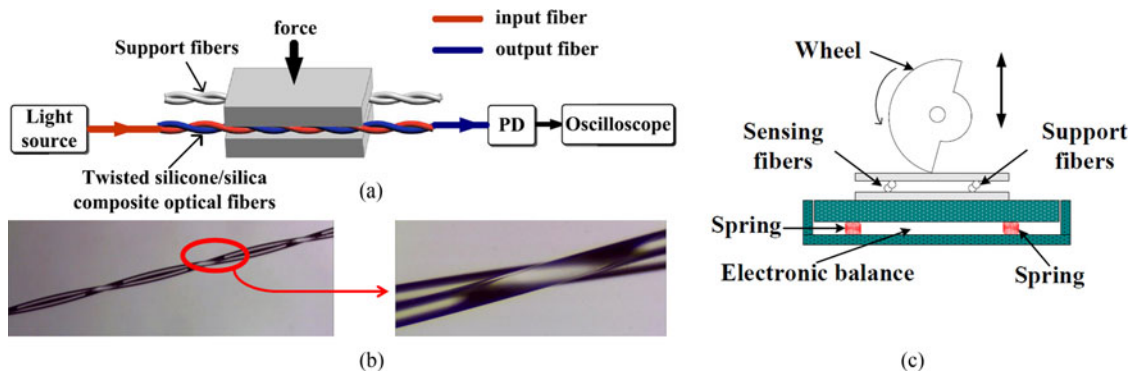


Fig. 2. (a) Experiment setup of using twisted silicone/silica composite optical fibers for side pressure sensing; (b) magnified image showing the fiber twisting of two composite optical fibers; (c) configuration of adding side pressure to the sensing fibers. PD: photodetector.

will be slightly changed by temperature, making the composite fiber also potential in temperature sensing. However, in this paper we focus on pressure sensing.

The experiment setup using the fabricated silicone/silica composite optical fibers for pressure sensing is shown in Fig. 2(a). Two composite fibers with the same length of 2.5 cm are twisted together with a small twisting pitch (2.5 mm) to serve as the sensing fibers. Fig. 2(b) shows the magnified images of the fiber twisting using two composite optical fibers. The purpose of twisting is to make the light coupling intensity stable and small pitch can make the pressure applied to the sensor uniform along the fibers, which ensures stable measurement [27], [28]. The sensing fibers together with support fibers are sandwiched between two glass plates, and the side pressure is applied from the top plate, as shown in Fig. 2(a). The support fibers are used for stable measurement. Optical light from a light source is injected into one of the twisted sensing fibers, i.e., input fiber in

Fig. 2(a). After the side pressure is applied from the top plate, the hyperelastic silicone claddings of the sensing fibers are compressed and the silica cores become close to each other, leading to the increase of light coupled from the input fiber to the other twisted sensing fiber, i.e., output fiber in Fig. 2(a). The light intensity coupled to the output fiber depends on the distance between the two fiber cores which is related to the applied side pressure. Thus by detecting the light intensity from the output fiber we can monitor the external side pressure applied to the sensing fibers. Here we use a photodetector and oscilloscope to detect the coupled light intensity for monitoring both static and dynamic side pressure. Fig. 2(c) illustrates how the side pressure is applied in our experiment. The two glass plates with sensing fibers and support fibers in between are fixed on top of an electronic balance which can measure and display the magnitude of side pressure applied to the top plate. The side pressure is generated through a wheel pressing the top plate and the magnitude of pressure can be changed by adjusting the vertical position of the wheel. To generate static side pressure the wheel is fixed; while to provide dynamic side pressure the wheel is driven by a motor to spin at a constant speed.

As the composite fiber is a multimode fiber, multimode interference exists and would lead to unstable intensity at a particular wavelength. In addition, the light coupling may take place at different positions of the twisted areas and cause multipath interference which would also give rise to unstable intensity. In order to minimize the fluctuation of coupled light intensity due to multimode and multipath interference, we use a broadband super-luminescent LED (SLED, Model DL-BX9-CS5169A, Denslight. Ltd) with 3-dB bandwidth of ~ 60 nm and output power of ~ 16 mW as the light source. With the use of broadband light source the effect of intensity fluctuation from multimode and multipath interference at each wavelength can be averaged and minimized to enhance the measurement stability. It is worth mentioning that we carefully align the composite fiber with a single mode fiber (SMF) and then splice them together which makes the composite fiber have a SMF pigtail and is connected to the SMF pigtail of the SLED. This makes fewer higher order modes excited. In addition, the propagation loss of composite fiber is larger compared with the silica fiber, especially for the higher order modes which have more optical power distributed at the silicone cladding region than the lower order modes, making them disappear after propagation for a shorter distance. Therefore higher order modes are not dominant inside this composite fiber and the multimode and multipath interference are further suppressed.

3. Results and Discussion

Before experiment, we first use simulation to compare the deformation of our silicone/silica composite optical fiber with conventional silica fiber and PMMA polymer fiber when they are under external force. Two-parameter Mooney-Rivlin model is used for simulation of the composite optical fibers (COMSOL, 2D structural mechanics model). The parameters for silicone in the simulation are set as follows: $C_{10} = 0.06 \times 10^6$, $C_{01} = 0.046 \times 10^6$, initial bulk modulus $k = 0.18 \times 10^6$, silicone density of 1272 kg/m^3 at room temperature. The Young's modulus and the Poisson's ratio are set to be 4.1878×10^6 Pa and 0.03769 for silicone, 7.30192×10^{10} Pa and 0.16707 for silica [29], 3×10^9 Pa and 0.37 for PMMA [30], respectively. The simulation results are given in Fig. 3. Fig. 3(a) shows the deformation of the composite fibers under different line forces. As the line force applied to the top glass plate increases, the hyperelastic silicone claddings are easily compressed and hence the silica cores become close to each other. The stronger the line force is, the larger the displacement of the fiber core distance between the two composite fibers is. This is more obvious from the red curve in Fig. 3(b) which depicts the displacement of the core distance for composite fiber as a function of line force. For comparison, the displacement for pure silica fiber and PMMA polymer fiber are also given as the dashed blue curve and dot green curve. The displacement of the core distance for composite fiber increases significantly as the line force increases; while the displacement for pure silica fiber and PMMA polymer fiber are almost unchanged when compared with the composite fiber, as indicated by the magnified view in the inset of Fig. 3(b). The Young's modulus of silicone is smaller than that of silica by four orders and PMMA by three orders, respectively. Thus the hyperelastic silicone claddings can be easily compressed to make the cores of composite

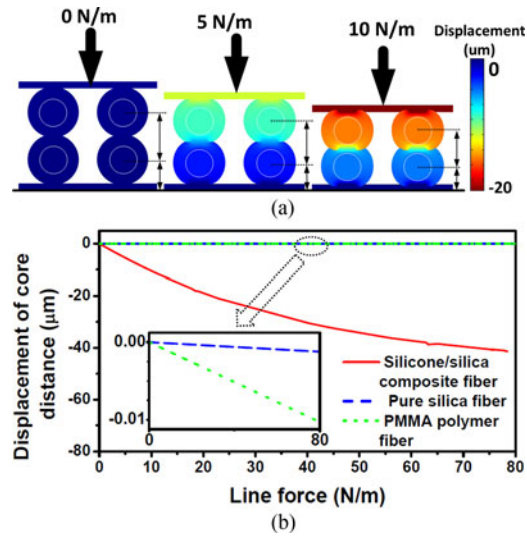


Fig. 3. (a) Deformation of the twisted composite fibers under different line forces; (b) displacement of the fiber core distance under different line forces. Inset: zoom-in view of the displacement for silica fiber and PMMA polymer fiber.

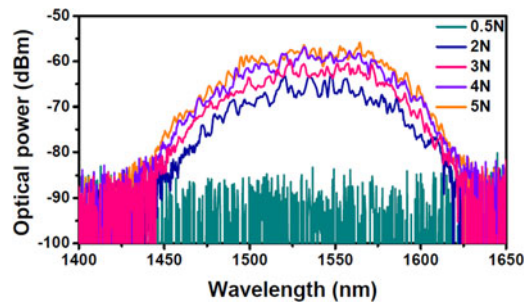


Fig. 4. Optical spectra of the coupled light under different static side pressures.

fibers approach each other even under small external force, enhancing the light coupling to realize high pressure sensitivity. While for the silica fiber and PMMA polymer fiber, the silica and PMMA polymer claddings are difficult to be compressed due to high Young's modulus, resulting in very small displacement and hence poor pressure sensitivity. According to [2], the silica fiber only has obvious response to external line force when the force is at the level of kN/m; while our composite fiber responds obviously even if the line force is three orders smaller, i.e., at a level of N/m, as shown in Fig. 3. Therefore, our composite fibers would be more sensitive to external pressure, even if the pressure is very small.

In order to demonstrate the high pressure sensitivity offered by our composite fibers, we apply static side pressure to the sensing fibers using the configuration in Fig. 2. Fig. 4 shows the optical spectra of the coupled light measured from the output fiber when the twisted composite fibers are under different static side pressures. No coupled light is observed under a side pressure of 0.5 N as shown by the green curve, since the fiber cores are too far away to have effective light coupling. As the side pressure increases, the light is coupled from the input fiber to the output fiber and corresponding optical spectra are observed. Larger side pressure results in stronger light coupling and hence higher intensity level of the spectrum, as shown in Fig. 4. Note that small ripples in the spectra originate from the multimode and multipath interference. Then we use the photodetector and oscilloscope to monitor the coupled light intensity as a function of static side pressure. The

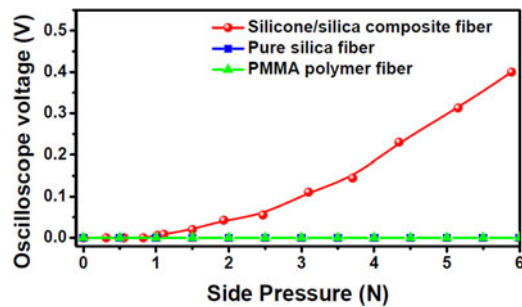


Fig. 5. Measured voltage on oscilloscope as a function of static side pressure.

voltage displayed on the oscilloscope is recorded, and the result is given as the red dots in Fig. 5. The voltage is kept almost zero when the side pressure is below 1 N. When the side pressure is beyond 1 N, the voltage increases significantly due to stronger light coupling. The coupled light intensity increases quite smoothly, which implies the effectiveness of minimizing intensity fluctuation by using broadband light source. From Fig. 5 we can see that the coupled light power is not a linear function of the side pressure. We calculate the percentage of nonlinearity of the curve defined as the maximum deviation from an ideal linear transfer function over the specified dynamic range. From the range of 3.5 N to 6 N in Fig. 5 the maximum percentage of nonlinearity is calculated to be 4.0%, which indicates a well linear region. While for the whole sensing range (i.e., 1 ~ 6 N) the maximum percentage of nonlinearity is calculated to be 20.5%. Here the polarization would not affect the sensor performance significantly as the output of the SLED is broadband unpolarized light. For comparison, we also measure the coupled light intensity when silica fiber (SMF-28, Corning Ltd.) and PMMA polymer fiber (EC-250, POFETH fiber) are employed for pressure sensing, respectively. The results are shown as blue rectangles and green triangles in Fig. 5. No voltage is observed for the cases of silica fiber and PMMA polymer fiber, which indicates that the two fibers are insensitive to such small pressure. While our composite fiber is highly sensitive to small pressure due to the low Young's modulus of its silicone cladding which strongly enhances the light coupling. The low Young's Modulus silicone has a medium ultimate tensile strength, e.g., 3.51–7.65 MPa [31], which makes the strength of the proposed composite fiber weaker than the normal fiber to some extent. There is a certain possibility that the fiber would be broken when the side pressure is larger than 6 N. Thus the composite fiber is a desirable candidate for highly sensitive small pressure monitoring. Note that we have repeated the measurement for several times, including the use of another two composite fibers of the same type, and it is found that our measurement is stable. This verifies the stability of our sensor and the stable light coupling by fiber twisting [28].

Next dynamic side pressure is applied to the composite sensing fibers and the same setup as shown in Fig. 2 is used to measure it. Periodic pressure with a period of ~ 2.4 s is applied and five different amplitudes (i.e., 0.5 N, 2 N, 3 N, 4 N, 5 N) are tested. Fig. 6(a) plots the measured voltage as a function of time on oscilloscope for different pressure levels. Due to the weak light coupling, no voltage is detected when the pressure amplitude is 0.5 N (red curve), which is consistent with the results in Fig. 4 and Fig. 5. For other pressure amplitudes, the voltage is measured to be a periodic function of time with almost the same period as that of the pressure applied to the sensing fibers, and the amplitude of voltage is proportional to that of the periodic pressure. The successful detection of dynamic pressure verifies the repeatability of the simple pressure sensor using light coupling from twisted composite optical fibers. The response time of the sensor can be estimated using the result of 5 N pressure amplitude in Fig. 6(a). The corresponding rising and falling time of the measured periodic signal are evaluated. The rising and falling time are defined as the time interval between 10% and 90% of the maximum voltage at the rising and falling edges, respectively, and they are estimated to be 0.12 s and 0.02 s, as shown in Fig. 6(b). Both the rising and falling time are much smaller than 1 s, implying fast response of the sensor for the purpose of rapid

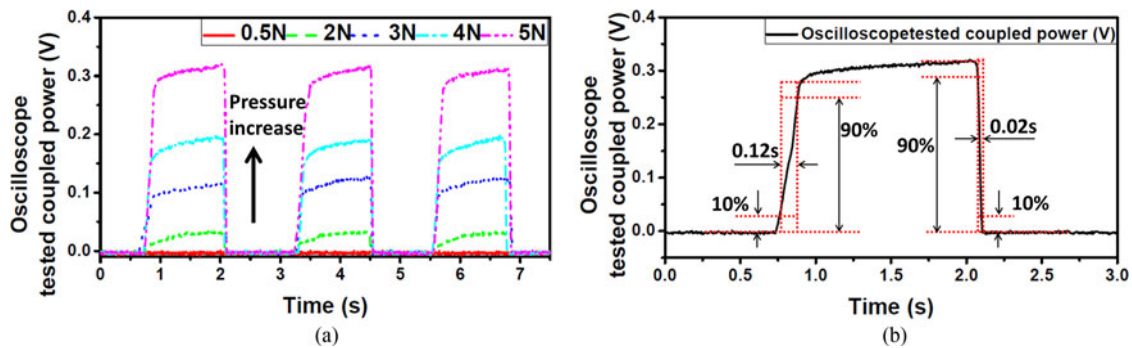


Fig. 6. (a) Measured voltage as a function of time on oscilloscope when periodic side pressure with different amplitudes are applied; (b) response time of the sensor based on light coupling from twisted silicone/silica composite optical fibers.

side pressure sensing. The rapid response can be attributed to the use of hyperelastic silicone material as the fiber cladding, as hyperelastic organic silicon materials, e.g., polydimethylsiloxane and silicone, usually exhibit relaxation time in the range of millisecond (~ 10 ms) when the pressure is completely released [17]–[19].

4. Conclusion

In conclusion, we have fabricated a composite optical fiber with hyperelastic silicone cladding and silica core and used it to monitor small side pressure at high sensitivity. A very simple pressure sensing configuration based on light coupling between two such composite fibers twisted together has been proposed and experimentally demonstrated. The soft silicone cladding has much smaller Young's modulus (e.g., three orders smaller than PMMA, four orders smaller than silica) which makes the fiber deformation easier under external pressure and hence improves the light coupling and pressure sensitivity. Simulation and experiment have been conducted to show the high pressure sensitivity offered by the composite fibers when compared with conventional silica fibers and PMMA polymer fibers. Both static and dynamic pressure with amplitude of several newtons have been successfully detected with excellent sensitivity and fast response time ($\ll 1$ s). The sensing scheme does not require any complicated fiber structures and would be a cost-effective way of monitoring small pressure at high sensitivity.

References

- [1] Z. Fang, K. K. Chin, R. Qu, and H. Cai, *Fundamentals of Optical Fiber Sensors*. Hoboken, NJ, USA: Wiley, 2012.
- [2] A. P. Zhang, B. O. Guan, X. M. Tao, and H. Y. Tam, "Experimental and theoretical analysis of fiber Bragg gratings under lateral compression," *Opt. Commun.*, vol. 206, no. 1–3, pp. 81–87, 2002.
- [3] W. Zhang, D. J. Webb, and G. D. Peng, "Investigation into time response of polymer fiber bragg grating based humidity sensors," *J. Lightw. Technol.*, vol. 30, no. 8, pp. 1090–1096, Apr. 2012.
- [4] Y. Lu, Z. Shen, C. Zhong, D. Chen, X. Dong, and J. Cai, "Refractive index and temperature sensor based on double-pass M–Z interferometer with an FBG," *IEEE Photon. Technol. Lett.*, vol. 26, no. 11, pp. 1124–1127, Jun. 2014.
- [5] L. Jin, B. O. Guan, and H. Wei, "Sensitivity characteristics of fabry-perot pressure sensors based on hollow-core microstructured fibers," *J. Lightw. Technol.*, vol. 31, no. 15, pp. 2526–2532, Aug. 2013.
- [6] L. Jin, Z. Quan, L. Cheng, and B.-O. Guan, "Hydrostatic pressure measurement with heterodyning fiber grating lasers: Mechanism and sensitivity enhancement," *J. Lightw. Technol.*, vol. 31, no. 9, pp. 1488–1494, May 2013.
- [7] Z. Li *et al.*, "Highly-sensitive gas pressure sensor using twin-core fiber based in-line Mach-Zehnder interferometer," *Opt. Exp.*, vol. 23, no. 5, pp. 6673–6678, 2015.
- [8] W. Talataisong, D. N. Wang, R. Chitaree, C. R. Liao, and C. Wang, "Fiber in-line Mach–Zehnder interferometer based on an inner air-cavity for high-pressure sensing," *Opt. Lett.*, vol. 40, no. 7, pp. 1220–1222, 2015.
- [9] J. Ma, J. Ju, L. Jin, and W. Jin, "A compact fiber-tip micro-cavity sensor for high-pressure measurement," *IEEE Photon. Technol. Lett.*, vol. 23, no. 21, pp. 1561–1563, Nov. 2011.

- [10] M. Yoon, S. Park, and Y. G. Han, "Simultaneous measurement of strain and temperature by using a micro-tapered fiber grating," *J. Lightw. Technol.*, vol. 30, no. 8, pp. 1156–1160, Apr. 2012.
- [11] K. Bhowmik *et al.*, "Experimental study and analysis of hydrostatic pressure sensitivity of polymer fibre bragg gratings," *J. Lightw. Technol.*, vol. 33, no. 12, pp. 2456–2462, Jun. 2015.
- [12] Y. Liu, Z. Guo, Y. Zhang, K. S. Chiang, and X. Dong, "Simultaneous pressure and temperature measurement with polymer-coated fiber Bragg grating," *Electron. Lett.*, vol. 36, no. 6, pp. 564–566, 2000.
- [13] Y. Zhang *et al.*, "High-Sensitivity pressure sensor using a shielded polymer-coated fiber bragg grating," *IEEE Photo. Technol. Lett.*, vol. 13, no. 6, pp. 618–619, Jun. 2001.
- [14] E. Pinet, "Pressure measurement with fiber-optic sensors: Commercial technologies and applications," *Proc SPIE*, vol. 7753, 2011, Art. no. 775304.
- [15] I. P. Johnson, D. J. Webb, and K. Kalli, "Hydrostatic pressure sensing using a polymer optical fibre Bragg gratings," *Proc. SPIE*, vol. 8351, 2012, Art. no. 835106.
- [16] G. Rajan, B. Liu, Y. H. Luo, E. Ambikairajah, and G. D. Peng, "High sensitivity force and pressure measurements using etched singlemode polymer fiber Bragg gratings," *IEEE Sensors J.*, vol. 13, no. 5, pp. 1794–1800, May 2013.
- [17] S. C. B. Mannsfeld *et al.*, "Highly sensitive flexible pressure sensors with microstructured rubber dielectric layers," *Nature Mater.*, vol. 9, pp. 859–864, 2010.
- [18] J. Lee *et al.*, "Conductive fiber-based ultrasensitive textile pressure sensor for wearable electronics," *Adv. Mater.*, vol. 27, no. 15, pp. 2433–2439, 2015.
- [19] Q. Wang, M. Jian, C. Wang, and Y. Zhang, "Carbonized silk nanofiber membrane for transparent and sensitive electronic skin," *Adv. Funct. Mater.*, vol. 27, no. 9, 2017, Art. no. 1605657.
- [20] A. Frutiger *et al.*, "Capacitive soft strain sensors via multicore-shell fiber printing," *Adv. Mater.*, vol. 27, no. 15, pp. 2440–2446, 2015.
- [21] O. Ziemann, J. Krauser, P. Zamzow, and W. Daum, *POF-Handbook – Short Range Optical Transmission Systems*, 2nd ed. New York, NY, USA: Springer-Verlag, 2008.
- [22] Y. Mizuno and K. Nakamura, "Potential of Brillouin scattering in polymer optical fiber for strain-insensitive high-accuracy temperature sensing," *Opt. Lett.*, vol. 35, no. 23, pp. 3985–3987, 2010.
- [23] R. Kruglov, J. Vinogradov, O. Ziemann, S. Loquai, and C. A. Bunge, "10.7-Gb/s Discrete Multitone Transmission Over 50-m SI-POF Based on WDM Technology," *IEEE Photon. Tech. Lett.*, vol. 24, no. 18, pp. 1632–1634, Sep. 2012.
- [24] R. Kruglov *et al.*, "21.4 Gb/s discrete multitone transmission over 50-m SI-POF employing 6-channel WDM," in *Proc. Opt. Fiber Commun. Conf. Exhib.*, San Francisco, CA, USA: Mar. 2014, Paper Th2A.2.
- [25] A. Othonos, "Fiber Bragg gratings," *Rev. Sci. Instrum.*, vol. 68, pp. 4309–4341, 1997.
- [26] C. Markos, K. Vlachos, and G. Kakarantzas, "Bending loss and thermo-optic effect of a hybrid PDMS/silica photonic crystal fiber," *Opt. Exp.*, vol. 18, no. 23, pp. 24344–24351, 2010.
- [27] A. W. Snyder, "Coupled-mode theory for optical fibers," *J. Opt. Soc. Amer.*, vol. 62, no. 11, pp. 1267–1277, 1972.
- [28] Y. L. Hou *et al.*, "Polymer optical fiber twisted macro-bend coupling system for liquid level detection," *Opt. Exp.*, vol. 22, no. 19, pp. 23231–23241, 2014.
- [29] L.C.S. Nunes, "Mechanical characterization of hyperelastic polydimethylsiloxane by simple shear test," *Mater. Sci. Eng.*, vol. 528, no. 3, pp. 1799–1804, 2011.
- [30] M. K. Szczurowski *et al.*, "Measurements of stress-optic coefficient and Young's modulus in PMMA fibers drawn under different conditions," *Proc. SPIE*, vol. 7741, 2010, Art. no. 77140G.
- [31] I. D. Johnston, D. K. McCluskey, C. K. L. Tan, and M. C. Tracey, "Mechanical characterization of bulk Sylgard 184 for microfluidics and microengineering," *J. Micromech. Microeng.*, vol. 24, no. 3, 2014, Art. no. 035017.